Chinese Chemical Letters 35 (2024) 109593

Contents lists available at ScienceDirect

Chinese Chemical Letters

journal homepage: www.elsevier.com/locate/cclet

Exceptional activity of amino-modified rGO-immobilized PdAu nanoclusters for visible light-promoted dehydrogenation of formic acid

Yiyue Ding[a], Qiuxiang Zhang[a], Lei Zhang[a], Qilu Yao[a,*], Gang Feng[b], Zhang-Hui Lu[a,*]

[a] Key Laboratory of Energy Catalysis and Conversion of Nanchang, College of Chemistry and Chemical Engineering, Jiangxi Normal University, Nanchang 330022, China
[b] School of Chemistry and Chemical Engineering, Nanchang University, Nanchang 330031, China

ARTICLE INFO

Article history:
Received 14 November 2023
Revised 29 January 2024
Accepted 30 January 2024
Available online 2 February 2024

Keywords:
Visible-light-enhanced
Hydrogen production
Formic acid
Pd-Au
Heterogeneous catalyst

ABSTRACT

Formic acid (FA), which is obtainable through CO_2 hydrogenation with green hydrogen or biomass conversion, has been used as a prospective liquid organic hydrogen carrier (LOHC) because of the abundant advantages of renewability, wide availability, stability, and high volumetric capacity (53 g H_2/L). The development of highly efficient catalytic systems to achieve enhanced catalytic activity is attractive but still challenging. Herein, ultrafine and highly dispersed PdAu nanoclusters (NCs) anchored on amino-modified reduced graphene oxide (ArGO) were successfully synthesized *via* a facile impregnation-reduction method and applied as a catalyst toward formic acid dehydrogenation (FAD). Benefiting from the promoting effect of amino groups, the strain and ligand effect in the alloy, and the Mott–Schottky effect between PdAu NCs and ArGO, the resultant PdAu/ArGO affords an ultrahigh activity under visible light irradiation with an exceptional turnover frequency value of 10,699.5 h^{-1} at 298 K without any additives, more than 2.6 times improvement than that under dark, which is the highest among all reported catalysts under the same conditions. This study provides a green and convenient strategy for developing more efficient and sustainable FAD catalysts and promotes the effective utilization of FA as a prospective renewable LOHC.

Hydrogen (H_2), as a green and sustainable energy carrier, has received unprecedented attention for its renewable nature and high energy density. However, safe transportation and controllable storage of H_2 still limit its widespread use [1]. Formic acid (FA, HCOOH), with the advantages of renewability, wide availability, stability, and high volumetric capacity (53 g H_2/L), has been used as a prospective liquid organic hydrogen carrier (LOHC) [2,3]. In particular, FA is obtainable through CO_2 hydrogenation with green H_2 or biomass conversion [4]. In the presence of a suitable catalyst, H_2 stored in FA can be released *via* a dehydrogenation pathway ($HCOOH \rightarrow CO_2 + H_2$) [5]. Therefore, the FA-CO_2 cycle can be achieved, by providing a comprehensive carbon-neutral H_2 storage system [6,7]. Nevertheless, this process is accompanied by a dehydration pathway ($HCOOH \rightarrow H_2O + CO$) that produces CO, which should be avoided for H_2 production [8–10].

Up to now, a lot of versatile heterogeneous catalysts have been investigated for formic acid dehydrogenation (FAD) [11–14]. However, most heterogeneous systems require elevated temperatures or extra additives to reach relatively high catalytic activity [15–17]. Therefore, a green and sustainable strategy is urgently needed to enable heterogeneous catalysts to maintain 100% H_2 selectivity at mild reaction temperature while greatly improving their catalytic activity and stability without the use of extra additives. Considering that solar energy is the most promising clean energy source, which reaches the earth composed of 43% visible light [18–22]. The development of visible light-assisted catalytic systems to achieve enhanced catalytic activity is considered an attractive way for FAD.

As reported, Pd [23,24], Au [11], and particularly Pd-Au alloys [15-17,25] are highly active for FAD. Recent theoretical and experimental results demonstrated that ultrafine metal nanoclusters (NCs) have better catalytic activity and/or selectivity than metal nanoparticles (NPs) because they have abundant corner and edge atoms that can expose more active sites. However, metal NCs tend to aggregate into larger NPs due to their high surface energy, leading to their rapid deactivation in catalytic applications [26]. Anchoring and dispersing metal NCs on a proper substrate can not only prevent their aggregation during the catalytic process, but also boost the catalytic activity of the catalyst through the strong electronic metal-support interaction (EMSI) [27,28]. Considering the potential of visible light-assisted enhancement of catalyst activity, integrating metals and semiconductor support to construct the Mott–Schottky structure is an effective method for

* Corresponding authors.
E-mail addresses: yaoqilu@jxnu.edu.cn (Q. Yao), luzh@jxnu.edu.cn (Z.-H. Lu).

https://doi.org/10.1016/j.cclet.2024.109593
1001-8417/

improving the catalytic performance [29–31]. Reduced graphene oxide (rGO) is an ideal substrate material with many advantages such as high electrical and thermal conductivity, excellent optical transparency, and large specific surface area. More importantly, it has been shown to have p-type semiconductor properties [32–34]. In addition, studies have shown that the hydrophilic amino groups ($-NH_2$) not only favor forming well-dispersed ultrafine active metal NCs, but also provide Brønsted basic sites for deprotonation of FA [35,36]. Therefore, highly active PdAu NCs anchored on amino-modified reduced graphene oxide (ArGO) are expected to display superior performance for FAD, and their activity can be further greatly enhanced under visible light irradiation *via* the Mott–Schottky effect.

Herein, ultrafine and highly dispersed PdAu NCs supported on ArGO were successfully synthesized through a facile impregnation-reduction method. Under visible light irradiation, the obtained PdAu/ArGO catalyst displays an exceptional catalytic performance with a high TOF of 10,699.5 h^{-1} for FAD at 298 K, which far exceeds that achieved under dark (4027.0 h^{-1}).

The fabrication process of PdAu/ArGO is illustrated in Fig. S1 (Supporting information). Firstly, AGO was prepared *via* a one-pot approach by mixing an aqueous GO solution with APTMS under magnetic stirring at room temperature. Subsequently, an aqueous solution containing Na_2PdCl_4 and $HAuCl_4{\cdot}3H_2O$ was introduced into the above mixture. PdAu/ArGO can be obtained rapidly by using $NaBH_4$ as a reducing agent. The detailed microscopic morphology of the as-prepared catalysts was investigated by transmission electron microscopy (TEM). TEM image displays that the PdAu NCs loaded on ArGO have very good dispersion with a very narrow particle size distribution of 1.5 nm (Fig. 1a). The Pd NCs loaded on ArGO also show excellent dispersion with a small particle size distribution of 1.7 nm (Fig. 1b). However, the rGO-supported PdAu NPs are bigger, with an average particle size of 2.7 nm (Fig. 1c), implying that ArGO is more conducive to dispersing NPs than rGO. This phenomenon can be attributed to the strong adsorption of metal ions by $-NH_2$ modified on GO, which favors the formation of very small and better-distributed metal NCs. The adsorption of Pd^{2+} and Au^{3+} cations by AGO was confirmed by ultraviolet−visible (UV–vis) spectra, as displayed in Fig. S2 (Supporting information). The presence of amino species in the catalysts can be verified by Fourier transform infrared spectroscopy (FT-IR) (Fig. S3 in Supporting information). Notably, the free PdAu NPs are severely aggregated and the particle size is about 5.7 nm (Fig. 1d), which is significantly larger than that of the PdAu NCs loaded on ArGO, implying that ArGO is an excellent support for dispersing NPs. HRTEM image of PdAu/ArGO shows a PdAu alloy structure with a lattice spacing of 0.229 nm (Fig. S4 in Supporting information). The XRD patterns show a peak located between Au (111) and Pd (111) appear in PdAu/ArGO (Fig. S5 in Supporting information), further confirming the formation of Pd-Au alloys.

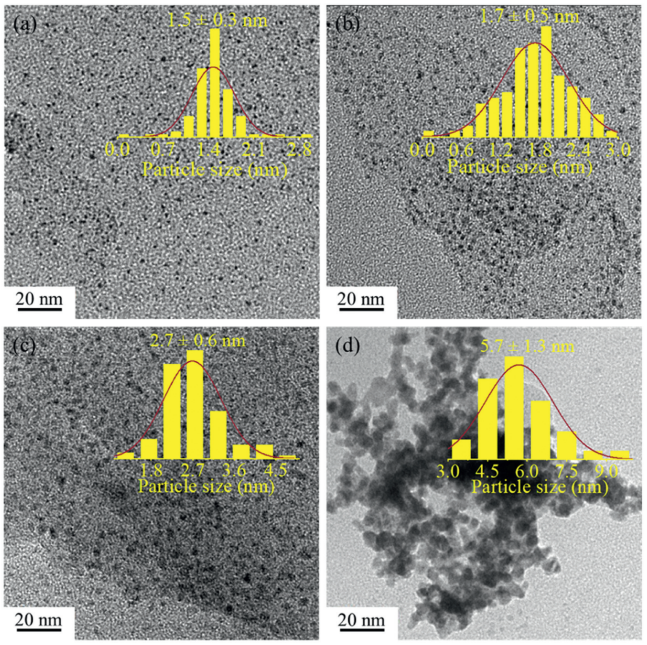

Fig. 1. TEM images of (a) PdAu/ArGO, (b) Pd/ArGO, (c) PdAu/rGO, and (d) PdAu NPs. The insets show the corresponding particle size distributions.

To investigate the chemical states and electronic effects of PdAu/ArGO and its relevant samples, X-ray photoelectron spectroscopy (XPS) measurements were applied. Comparing PdAu/ArGO with pure PdAu NPs, both the Pd 3d peak and the Au 4f peak in PdAu/ArGO slightly shift to lower binding energies (BEs) (Figs. S6a and b in Supporting information), confirming the transfer of some electrons from ArGO to PdAu NCs through the EMSI. The N 1s peak of PdAu/ArGO shifts to a higher BE by 0.12 eV (from 399.18 eV to 399.30 eV) and 0.47 eV (from 398.83 eV to 399.30 eV) compared to the monometallic Pd/ArGO and Au/ArGO catalysts, respectively (Fig. S6c in Supporting information), suggesting that $-NH_2$ can be used as the electron donor to optimize the electronic structure of active metal NPs. Moreover, the Pd 3d peak shifts to higher BEs and the Au 4f peak shifts to lower BEs for PdAu/ArGO compared to Pd/ArGO and Au/ArGO. These shifts might be attributed to the unique electronic coupling and charge redistribution between Pd and Au induced by lattice strain and ligand effects in the alloy. Therefore, the resulting electron-rich PdAu active sites with the optimized electronic structure can stimulate the cleavage of C–H bonds in the absorbed HCOO* intermediates on the catalyst and thereby accelerate FAD [29-31,37].

The photoabsorption properties of different samples were studied by UV–vis absorption spectroscopy. As presented in Fig. 2a, GO exhibits weak visible light absorption. After amino modification, the range of light absorption of GO is broadened from UV to visible region, which indicates that effective amino modification can significantly expand the light absorption range of GO and facilitate the absorption and utilization of light energy by the catalyst. Moreover, it can be easily observed that PdAu/ArGO has good absorption of visible light. The separation and transfer efficiency of photogenerated charge carriers in different samples were analyzed by static photoluminescence (PL) spectroscopy and photocurrent density measurements. As shown in Fig. 2b, the intensity of the PL emission peak of GO is greatly weakened by the introduction of amino modification, suggesting a faster charge transfer in AGO compared to GO. Especially, the intensity of the AGO emission peak decreases significantly after the formation of the metal catalyst. This suggests that the metal-semiconductor heterojunction structure constructed between metal NCs and ArGO significantly suppresses the radiative recombination of photogenerated charge carriers through the Mott–Schottky effect [29,30]. In this structure, electrons transfer from the ArGO to metal NCs, as confirmed by XPS (Fig. S6). Moreover, PdAu/ArGO shows the highest photocurrent density under visible light irradiation compared with other samples (Fig. 2c). The photocurrent density of PdAu/ArGO is about 1.8 times higher than that of AGO, indicating that the photogenerated charge carriers may be rapidly separated by electron transfer from ArGO to PdAu NCs, which is consistent with the PL results. In addition, electrochemical impedance spectroscopy (EIS) measurements show that the charge transfer resistance is in the order of GO > AGO > PdAu/ArGO (Fig. 2d). The small charge transfer resistance of PdAu/ArGO suggests that electrons can be easily transferred from the surface of the catalysts to the reactants or the acceptors of the photogenerated electrons, which improves the ef-

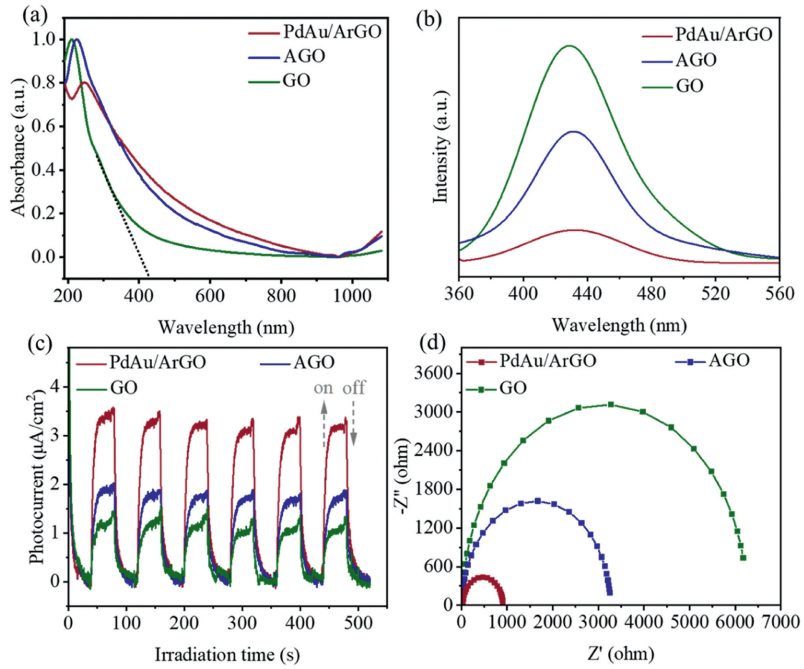

Fig. 2. (a) Normalized UV–vis absorption spectra of different samples dispersed in water (0.05 mg/mL). (b) PL spectra, (c) time *versus* transient photocurrent density curves, and (d) EIS spectra of different samples.

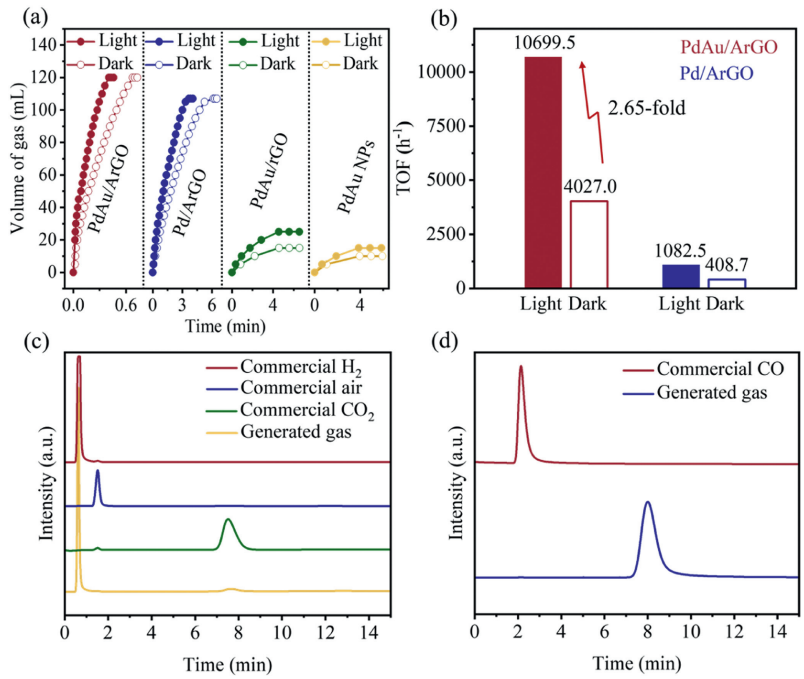

Fig. 3. (a) Volume of generated gas ($H_2 + CO_2$) *versus* time for FAD over different catalysts under light and dark at 298 K. (b) The corresponding TOF values. GC spectra using (c) TCD detector and (d) FID-methanator for the commercial gas and the generated gas from FAD over PdAu/ArGO under light at 298 K.

ficiency of the catalytic reaction. Based on the aforementioned results, it is expected that PdAu/ArGO will exhibit significantly enhanced catalytic activity toward FAD under visible light, which can be immediately evidenced by subsequent catalytic results.

The catalytic performances of the prepared catalysts were investigated in FA aqueous solution by monitoring the volume and time of gas ($H_2 + CO_2$) generation. As shown in Fig. 3a, the PdAu/ArGO displays an excellent activity for FAD with a TOF of 4027.0 h^{-1} at 298 K, which is comparable to the state-of-the-art reported PdAu-based catalysts [16,17]. Moreover, the activity of PdAu/ArGO for FAD can be further greatly improved by visible light irradiation with a high TOF of 10,699.5 h^{-1} at 298 K (Fig. 3b), which is 2.6 times higher than that achieved under dark (4027.0 h^{-1}) and is the highest among all reported catalysts under the same conditions (Table S1 in Supporting information). Gas chromatography (GC) analysis confirms that the gas released is only H_2 and CO_2 with no CO (Figs. 3c and d), indicating PdAu/ArGO possesses 100% H_2 selectivity for FAD. Similarly, a significant acceleration of its H_2 release rate is also observed in Pd/ArGO under visible light. The enhanced catalytic activity can be attributed to the large num-

ber of electrons generated by ArGO after photoexcitation transfer to the active NCs, and the obtained electron-rich active sites can facilitate the cleavage of C–H bonds in FA molecules, thereby greatly improving the catalytic efficiency [29-31,37]. The higher catalytic activity of PdAu/ArGO than that of Pd/ArGO can be attributed to the strong electronic coupling and charge redistribution between Pd and Au (Fig. S6). As shown in Fig. S7 (Supporting information), the different Pd and Au compositions of Pd_xAu_{1-x}/ArGO can significantly affect its performance. The highest performance of Pd_xAu_{1-x}/ArGO is achieved when the molar ratio of Pd/Au is 0.6/0.4. In addition, the correlation between the performance and the loading of active metal NCs was also investigated (Fig. S8 in Supporting information). The PdAu/ArGO displays the best performance when the amount of GO is 18 mg and the corresponding metal loading is 23.9 wt% according to the ICP-OES test results.

In contrast, both PdAu/rGO and free PdAu NPs have poor catalytic activity for FAD, and their activity under visible light irradiation is improved compared to that under dark (Fig. 3a). In addition, compared with free PdAu NPs, the catalytic activity of PdAu/rGO is slightly improved, but still far inferior to that of PdAu/ArGO catalyst. The above results indicate that the introduction of $-NH_2$ is of great significance in improving the catalytic activity, and its role is mainly reflected in the following aspects. Firstly, $-NH_2$ can efficiently adsorb metal ions and control the nucleation and growth of NPs, thereby promoting the formation of ultrasmall and uniformly dispersed metal NCs with more exposed active sites (Fig. 1a and Fig. S2). Secondly, $-NH_2$ can act as Brønsted basic sites to promote FAD (Fig. S9 in Supporting information). This promoting process of $-NH_2$ for breaking of O–H bond of FA is demonstrated by theoretical calculations using the density functional theory (DFT) methods [35,36]. Fig. S10 (Supporting information) confirms that PdAu/ArGO has a higher concentration of basic sites than PdAu/rGO, which is very favorable for the deprotonation of FA. Moreover, $-NH_2$ can act as the electron donor to optimize the electronic structure of active metal NPs (Fig. S6c), and the resulting electron-rich PdAu active sites can stimulate the cleavage of C–H bonds in the absorbed HCOO* intermediates on the catalyst and thereby accelerate FAD [29-31,37]. In addition, $-NH_2$ can broaden the light absorption range of GO (Fig. 2a), which is favorable for absorbing and utilizing light energy by the catalyst.

The dehydrogenation reactions catalyzed by PdAu/ArGO and Pd/ArGO were carried out under light and dark at different temperatures (298–328 K). The reaction rate rises with increasing reaction temperature (Fig. 4a and Fig. S11 in Supporting information). According to the Arrhenius equation, the apparent activation energies of PdAu/ArGO and Pd/ArGO under light are calculated to be 15.1 and 39.7 kJ/mol, respectively, which are much lower than their apparent activation energies under dark (32.0 and 47.4 kJ/mol) (Fig. 4b). This is probably because catalysts can be excited by visible light to produce more photogenerated charge carriers to trigger their reactions with FA molecules, which means that the reaction requires "less energy" to overcome the activation barrier. In addition, the lower activation energy of PdAu/ArGO compared to Pd/ArGO may be due to the strong electronic coupling and charge redistribution between Pd and Au, which enhances the interactions between the active PdAu NCs and FA molecules. The activation energy of PdAu/ArGO under light (15.1 kJ/mol) is the lowest value reported so far (Fig. 4c), reflecting its excellent kinetic superiority for FAD.

We further investigated the durability of PdAu/ArGO for FAD. PdAu/ArGO shows 100% H_2 selectivity and conversion in the durability tests under both light and dark, but the gas release rate decreases after ten cycles (Fig. 4d and Fig. S12 in Supporting information). It can be observed that the degree of activity decay under light is greater than that under dark, although the gas release rate in the tenth cycle is faster, suggesting that the addition of visible light irradiation promotes the activity decay of the catalyst. After the durability test, the catalyst was characterized by XRD, TEM, XPS, FT-IR, and EA analysis. The XRD patterns show no change in the phase structure of the reused catalyst (Fig. S13 in Supporting information). TEM images reveal that the PdAu NCs remain well dispersed after ten reaction cycles, but the particle size increases

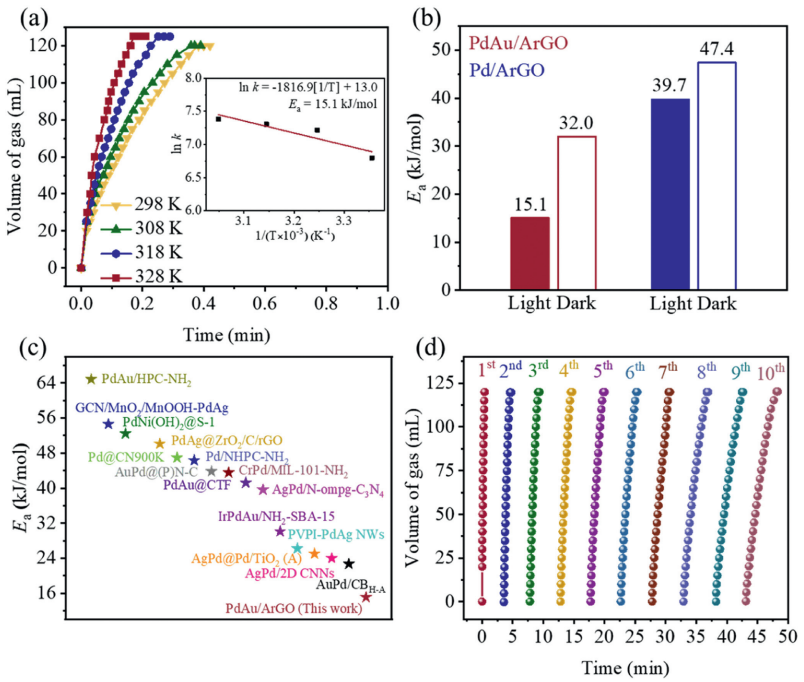

Fig. 4. (a) Volume of generated gas ($H_2 + CO_2$) *versus* time for FAD over PdAu/ArGO under light at different temperatures. The inset shows the corresponding Arrhenius plot. (b) The apparent activation energy of different catalysts. (c) Comparison of the apparent activation energy of our PdAu/ArGO catalyst with other reported catalysts. (d) Durability test for FAD over PdAu/ArGO under light at 298 K.

slightly (1.8 nm) (Fig. S14 in Supporting information). As shown from XPS in Fig. S15 (Supporting information), the chemical state of noble-metal species remains almost unchanged. In addition, FT-IR spectra (Fig. S16 in Supporting information) and EA tests (Table S2 in Supporting information) confirm that the amino components in the catalyst decrease after cycling. The increase in the size of the active PdAu NCs and the decrease in the concentration of surface $-NH_2$ of the catalyst may be the main reasons for the decrease in activity.

In summary, the PdAu/ArGO catalyst was successfully synthesized through a facile impregnation-reduction method and further applied for rapid FAD. The prepared PdAu/ArGO catalyst displays an ultrahigh performance under visible light irradiation with a TOF of 10,699.5 h^{-1} at 298 K without any additives, which is much higher than that achieved under dark (4027.0 h^{-1}) and is the highest among all reported catalysts under the same conditions. The sharply enhanced activity of PdAu/ArGO under visible light irradiation is mainly derived from a synergistic combination of the promoting effect of $-NH_2$, the lattice strain and ligand effect in the alloy, and the Mott–Schottky effect between PdAu NCs and ArGO, which promotes the formation of electron-rich, ultrafine, and highly dispersed active PdAu NCs. Furthermore, this catalyst possesses excellent kinetic superiority for FAD under visible light irradiation with a calculated apparent activation energy of 15.1 kJ/mol, which is the lowest value reported so far. This study provides a green and convenient strategy for developing more efficient and sustainable FAD catalysts and promotes the effective utilization of FA as a prospective renewable LOHC.

Declaration of competing interest

The authors declare that they have no known competing financial interests or personal relationships that could have appeared to influence the work reported in this paper.

Acknowledgments

This work was financially supported by the National Natural Science Foundation of China (Nos. 22162014 and 22162013) and Department of Science and Technology of Jiangxi Province (Nos. 20212ACB204009, 20212BCJL23059 and 20232ACB214002).

Supplementary materials

Supplementary material associated with this article can be found, in the online version, at doi:10.1016/j.cclet.2024.109593.

References

[1] Q. Yao, X. Zhang, Z.H. Lu, et al., Coord. Chem. Rev. 493 (2023) 215302.
[2] Q. Sun, N. Wang, Q. Xu, et al., Adv. Mater. 32 (2020) e2001818.
[3] O. Altan, E. Altintas, S. Alemdar, et al., Chem. Eng. J. 441 (2022) 136047.
[4] T. Wang, L. Yang, D. Jiang, et al., ACS Appl. Mater. Interfaces 13 (2021) 23751–23759.
[5] F. Valentini, V. Kozell, C. Petrucci, et al., Energy Environ. Sci. 12 (2019) 2646–2664.
[6] X. Li, A.E. Surkus, J. Rabeah, et al., Angew. Chem. Int. Ed. 59 (2020) 15849–15854.
[7] W. Peng, S. Liu, X. Li, et al., Chin. Chem. Lett. 33 (2022) 1403–1406.
[8] Y. Luo, Q. Yang, W. Nie, et al., ACS Appl. Mater. Interfaces 12 (2020) 8082–8090.
[9] W. Gao, Q. Liu, X. Zhao, et al., Nano Energy 80 (2021) 105543.
[10] W.F. Peng, X. Sun, Y. Ding, et al., ACS Sustain. Chem. Eng. 11 (2023) 1898–1908.
[11] H. Liu, H. Zou, D. Wang, et al., Angew. Chem. Int. Ed. 62 (2023) e202216739.
[12] A. García-Baldoví, R. Del Angel, G. Mouchaham, et al., Energy Environ. Sci. 16 (2023) 167–177.
[13] A. Gemenetzi, Y. Deligiannakis, M. Louloudi, ACS Catal. 13 (2023) 9905–9917.
[14] R.M. Irfan, T. Wang, D. Jiang, et al., Angew. Chem. Int. Ed. 59 (2020) 14818–14824.
[15] P. Liu, X. Gu, H. Zhang, et al., Appl. Catal. B 204 (2017) 497–504.
[16] Y. Cui, M. Zhao, Y. Zou, et al., J. Energy Chem. 68 (2022) 556–563.
[17] S.J. Li, Y.T. Zhou, X. Kang, et al., Adv. Mater. 31 (2019) e1806781.
[18] X. Bai, S. Li, Y. Zhang, et al., Green Chem. 23 (2021) 7630–7634.
[19] M. Herran, A. Sousa-Castillo, C. Fan, et al., Adv. Funct. Mater. 32 (2022) 2203418.
[20] H. Issa Hamoud, P. Damacet, D. Fan, et al., J. Am. Chem. Soc. 144 (2022) 16433–16446.
[21] S. Zhang, S. Duan, G. Chen, et al., Chin. J. Catal. 42 (2021) 193–204.
[22] P. Zhou, Q. Zhang, Z. Xu, et al., Adv. Mater. 32 (2020) 1904249.
[23] Z. Chen, C.A.M. Stein, R. Qu, et al., ACS Catal. 13 (2023) 4835–4841.
[24] Z. Zhang, Y. Luo, S. Liu, et al., J. Mater. Chem. A 7 (2019) 21438–21446.
[25] X. Sun, Y. Ding, G. Feng, et al., J. Colloid Interface Sci. 645 (2023) 676–684.
[26] Q. Meng, X. Wang, M. Xiao, et al., Chin. Chem. Lett. 34 (2023) 107221.
[27] R. Li, Z. Liu, Q.T. Trinh, et al., Adv. Mater. 33 (2021) 2101536.
[28] X. Du, Y. Huang, X. Pan, et al., Nat. Commun. 11 (2020) 5811.
[29] S. Zhang, M. Li, J. Zhao, et al., Appl. Catal. B 252 (2019) 24–32.
[30] C. Wan, L. Zhou, L. Sun, et al., Chem. Eng. J. 396 (2020) 125229.
[31] H. Liu, X.X. Li, X.Y. Liu, et al., Rare Metals 40 (2021) 808–816.
[32] C. Chen, W. Cai, M. Long, et al., ACS Nano 4 (2010) 6425–6432.
[33] A. Khan, B. Nilam, C. Rukhsar, et al., Tungsten 5 (2022) 391–418.
[34] Q.L. Yao, M. He, Y.R. Kong, et al., Rare Metals 42 (2023) 3410–3419.
[35] S. Masuda, K. Mori, Y. Futamura, et al., ACS Catal. 8 (2018) 2277–2285.
[36] W. Ye, W. Pei, S. Zhou, et al., J. Mater. Chem. A 7 (2019) 10363–10371.
[37] J. Zhu, J. Huang, J. Dai, et al., ChemSusChem 16 (2023) e202202069.